Article Chinese Science Bulletin

SPECIAL TOPIC October 2013 Vol.58 No.28-29: 3451–3459
Coseismic Deformation and Rupture Processes of the 2013 Lushan Earthquake doi: 10.1007/s11434-013-6000-2

Relocation of the mainshock and aftershock sequences of M_S7.0 Sichuan Lushan earthquake

FANG LiHua[1], WU JianPing[1*], WANG WeiLai[1], LÜ ZuoYong[2], WANG ChangZai[1], YANG Ting[1] & CAI Yan[1]

[1] *Institute of Geophysics, China Earthquake Administration, Beijing 100081, China;*
[2] *Guangdong Earthquake Administration, Guangzhou 510070, China*

Received June 7, 2013; accepted June 24, 2013; published online July 25, 2013

The mainshock of April 20, 2013 Sichuan Lushan M_S7.0 earthquake was relocated using a 3-D velocity model. Double difference algorithm was applied to relocate aftershock sequences of Lushan earthquake. The locations of 2405 aftershocks were determined. The location errors in E-W, N-S and U-D direction were 0.30, 0.29 and 0.59 km on average, respectively. The location of the mainshock is 102.983°E, 30.291°N and the focal depth is 17.6 km. The relocation results show that the aftershocks spread approximately 35 km in length and 16 km in width. The dominant distribution of the focal depth ranges from 10 to 20 km. A few earthquakes occurred in the shallow crust. Focal depth profiles show fault planes dip to the northwest, manifested itself as a listric thrust fault. The dip angle is steep in the shallow crust and gentle in the deep crust. Although the epicenters of aftershocks distributed mainly along both sides of the Shuangshi-Dachuan fault, the seismogenic fault may be a blind thrust fault on the eastern side of the Shuangshi-Dachuan fault. Earthquake relocation results reveal that there is a southeastward tilt aftershock belt intersecting with the seismogenic fault with y-shape. We speculate it is a back thrust fault that often appears in a thrust fault system. Lushan earthquake triggered the seismic activity of the back thrust fault.

Lushan earthquake, aftershock sequence, earthquake location, double difference location, Longmenshan fault

Citation: Fang L H, Wu J P, Wang W L, et al. Relocation of the mainshock and aftershock sequences of *M*s7.0 Sichuan Lushan earthquake. Chin Sci Bull, 2013, 58: 3451–3459, doi: 10.1007/s11434-013-6000-2

At 08:02 am on April 20, 2013 (Beijing time), a strong earthquake (M_S7.0) occurred in Lushan County, Sichuan Province (hereafter referred to as Lushan earthquake). The location of the mainshock determined by China Earthquake Network Center is 30.3°N, 103.0°E and the focal depth is 13 km. According to the statistics from Sichuan Earthquake Administration, 3811 aftershocks were recorded by the end of 12:00 am on April 27, 8 of which had magnitude larger than M_L5.0. The 193 people were killed, 25 people were missing and more than ten thousand people were injured in the earthquake. Direct economic losses were estimated to be more than ten billion yuan (RMB).

Lushan earthquake is another devastating earthquake that occurred in Sichuan Province after May 12, 2008 M_S8.0 Wenchuan earthquake. Lushan earthquake occurred in the southern part of the Longmenshan fault zone. The distance between the epicenters of these two earthquakes is about 87 km. There is an aseismic zone between the two aftershock areas. The length scale of the aseismic zone is about 45 km. Three earthquakes with magnitude lager than *M*6.0 occurred at the southern section of the Longmenshan fault in history. These strong earthquakes are Tianquan earthquake in 1327, Baoxing-Kangding *M*6.0 earthquake on June 12, 1941 and Dayi *M*6.2 earthquake on February 2, 1970 [1].

The Longmenshan fault system was formed in the Mesozoic orogeny. This fault zone is a major active fault about 500 km long and 40–50 km wide, which shows dextral strike-slip-thrust movement characteristics. The Longmenshan fault has the strike of N40°–50°E and dips to northwest. The fault system is consisted of four main faults (Fig-

*Corresponding author (email: wjpwu@cea-igp.ac.cn)

ure 1), from northwest to southeast as follows: the back fault, central fault, front fault and blind fault [2–12].

The Institute of Geophysics, China Earthquake Administration started the emergency response promptly after Lushan earthquake. We immediately conducted relocation of the mainshock and aftershock sequences. The updated relocation results were released and reported to China Earthquake Administration via email and other relevant channels. We relocated the mainshock using 'Sichuan-Yunnan traveltime table earthquake location software' and a 3-D velocity model. We relocated the aftershock sequences using the double difference location algorithm. The relocation results provide important reference for earthquake emergency rescue, research of Lushan seismogenic structure, analysis of spatial and temporal characteristics of aftershock activity, as well as determination of the trends of aftershock activity.

1 Station and data

1.1 Station information

Before the Lushan earthquake, there were 27 permanent seismic stations in service with epicentral distances less than 200 km. Among them, the epicentral distance of three stations is less than 35 km, namely Baoxing station, Ya'an station and Tianquan station. The epicentral distance of the three stations is 18, 27 and 32 km, respectively. This three near stations provided good azimuthal coverage and played important roles in the early stage earthquake locations. After the mainshock, the data transformation of Baoxing station was stopped due to the communication malfunction. Baoxing station was repaired at 13:00 pm on April 21.

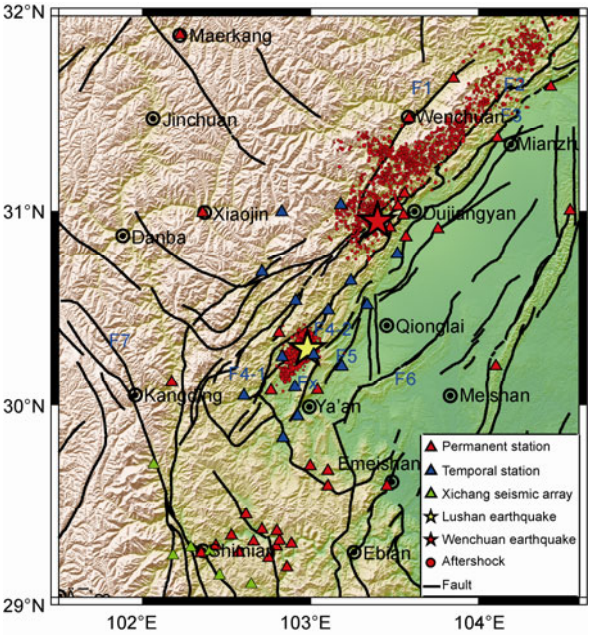

Figure 1 Distribution of seismic stations and faults. Red triangles indicate permanent seismic stations, blue triangles for temporal stations deployed after Lushan earthquake, green triangles for Xichang Array stations. Yellow and red stars represent epicenters of Lushan earthquake and Wenchuan earthquake, respectively. Red circles indicate aftershocks of Lushan earthquake and Wenchuan earthquake. The main faults are: F1, Wenchuan-Maowen fracture; F2, Beichuan-Yingxiu fault; F3, Jiangyou-Guanxian fault; F4-1, Shuangshi-Dachuan main fault; F4-2, Shuangshi-Dachuan branch fault; F5, Dayi fault; F6, Pujiang-Xinjin fault; F7, Xianshuihe fault; Fx, unknown fault. Fault data are from the fifth edition of the national zoning map of ground motion[1)] and Xu et al. [13].

According to the coordination of China Earthquake Administration, Institute of Geophysics, Yunnan Earthquake Administration, Chongqing Earthquake Administration, Hubei Earthquake Administration, and Sichuan Earthquake Administration started to install temporal stations around the earthquake area. By the end of April 25, 15 temporal seismic stations were installed (Figure 1). The epicentral distances of these temporal stations are less than 50 km. The waveform data were transferred to Sichuan Earthquake Administration in real time. The waveform data of the temporal and permanent seismic stations are processed uniformly in Sichuan Earthquake Network Center. As shown in Figure 1, temporal and permanent seismic stations cover the aftershock region very well, ensuring the reliability of earthquake location results.

1.2 Data

After the earthquake, China Earthquake Administration immediately selected technical backbones from Guangdong Earthquake Administration, Hebei Earthquake Administration, Jiangsu Earthquake Administration, Yunnan Earthquake Administration, Shandong Earthquake Administration and other units to go to Chengdu. They helped Sichuan Earthquake Administration to process the aftershock sequences, ensuring the production of Lushan aftershock observation report timely. The phase data and the initial earthquake location results used in this study are mainly from the observation report of Sichuan Earthquake Administration, which were checked and summarized uniformly by the China Earthquake Networks Center.

By the end of 12:00 am on April 27, 2013, 3811 aftershocks were analyzed by Sichuan Earthquake Administration. The magnitude ranges from M_L0.0 to M_L5.5. Figure 2 shows distributions of the epicenters and focal depths along the longitude and latitude. In this study, we only relocate aftershocks with magnitude larger than M_L1.0 and phase number larger than 8. The phase data used in the relocation are mainly from 71 stations with epicentral distance less than 200 km. We plotted the P-wave and S-wave traveltime curves to check the reliability of the phase data. As shown from Figure 3, Pg and Sg traveltime curves can be clearly distinguished from each other, and the deviation of traveltime

1) Editorial Board of National Seismic Zoning Map. Ground Motion Parameter Zoning Map of China (replace for GB 18306-2001). 2013

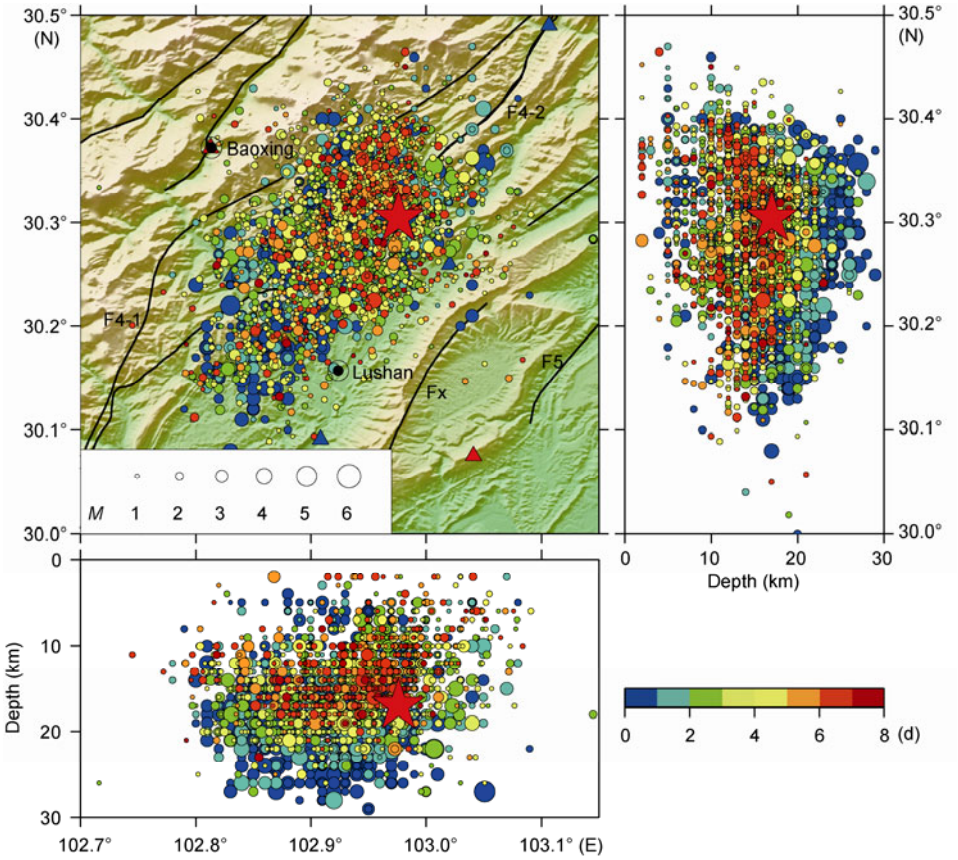

Figure 2 Distributions of initial epicenter and focal depth profiles along the longitude and latitude. The data are from observation reports of Sichuan Earthquake Administration. Red star represents the location of mainshock. Circles represent aftershocks with magnitude proportional to its size. The color of the circles changes with time from blue to red (Unit of color scale: d).

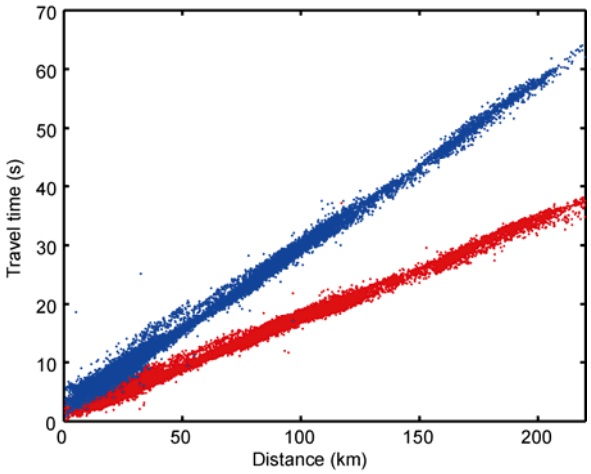

Figure 3 Traveltime curves. Red and blue dots represent traveltime of Pg and Sg phases.

is small, indicating that the phase data are reliable.

2 Method

The observation data used in this study are from regional seismic network in Sichuan, Chongqing, Yunnan, Xichang seismic array, and 15 temporal seismic stations installed after the earthquake. At first, we used LOC3D (Sichuan-Yunnan traveltime table earthquake location software) to determine the location of the mainshock, and then relocated aftershocks with Hypo2000 to obtain the absolute locations. Finally, we relocated aftershocks with double difference location algorithm to enhance the location precision.

2.1 Mainshock relocation

We relocated the mainshock of Lushan earthquake using the waveform data provided by Data Backup Center of National Digital Seismic Network [14] with 'Sichuan-Yunnan traveltime table earthquake location software' [15,16]. The software takes into account the earth ellipticity, station elevation, topography and other factors, and is based on 3-D velocity discontinuities and 3-D velocity model. It can use a variety of regional earthquake phases. The inversion algorithm is a simplex method.

When locating the mainshock, in addition to using the waveform data of the regional seismic network in Yunnan, Sichuan and Chongqing, we also used the waveform data of Xichang seismic array deployed by our research group. Xichang seismic array effectively improved the azimuth

coverage in southwest direction, making the location results more reliable.

We chose the stations with high signal to noise ratio, clear phases and good azimuth coverage to mark phase arrivals. Finally we used 57 stations and 70 phases to relocate the mainshock, including 31 Pg phases, 25 Pn phases and 14 Sg phases. The coordinate of the mainshock is 102.981°E, 30.303°N and the focal depth is 17.2 km after relocation. Horizontal and vertical location errors are 0.4 and 0.6 km, respectively.

2.2 Absolute relocation of aftershocks

Sichuan Earthquake Administration uses LOC3D, Hypo2000 and simplex method in initial earthquake location. Different location methods may give different results with systematic biases due to the difference of velocity model and parameters used in the location. In order to improve the accuracy of initial focal location, we relocated aftershocks with Hypo2000 in the first step. After Hypo2000 absolute location, the average location residuals reduce to 0.29 s and the distribution of focal depth is more concentrated.

The velocity structure used in relocation is modified from Wang et al. [17] (referred to as model A) and Zhao et al. [18] (referred to as model B, Table 1). The location results from the two models are basically similar, but the location residual and error using model A are less than that of model B. In addition, model A is from deep seismic sounding results, and near the aftershock zone, so we use model A in absolute and relative location. The receiver function studies in this region show that the *V*p/*V*s ratio near the aftershock zone is relatively high. The *V*p/*V*s ratio is set to 1.83 according to the results of receiver function *h*-*k* of Wang et al. [19].

2.3 Relative relocation of aftershocks

In this study we apply the double difference location algorithm to obtain the relative locations of aftershocks [20]. This method uses the traveltime differences to invert for hypocenter locations. It can eliminate ray path effects from different sources to same stations effectively and depends weakly on the crustal velocity model. The location accuracy is on an order of hundred meters in a small area. Recently, the method has been widely applied to earthquake relocation at home and abroad [21–27]. The temporal stations installed after the earthquake are quite intensive, and may cause systematic change to the location results after the temporal stations were set up compared with the results before. In this research, we correct the location of early aftershocks using the aftershocks relocation results after temporal stations set up.

Table 1 1-D velocity model used in earthquake relocation

Model A		Model B	
P-wave velocity (km s^{-1})	Depth (km)	P-wave velocity (km s^{-1})	Depth (km)
5.30	0	4.88	0
6.05	4	5.80	3
6.35	17	6.04	8
6.75	28	6.82	22
7.00	39	7.61	43
8.15	45	8.15	69

There are 2465 events with magnitude larger than 1.0 and phase number greater than 8. There are 46772 earthquake phases, 24636 of which are P-wave phases and 22136 of which are S-wave phases. On average, each event has 19 phase arrival data (about 10 stations). The initial location residual is 0.35 s on average, and focal depth distributes from 0 to 36 km.

To find neighboring events, we set the minimum number of links required to define a neighbor (MINLNK) and the minimum number of per pair (MINOBS) to 8, the maximum hypocentral separation between event pairs to 10 km, and maximum distance between pair and station to 220 km. We give a weight of 1.0 for P-wave data and 0.7 for S-wave data during relocation. The iteration has ten times and is grouped into three sets. We use four times of the standard deviations as the cutoff value in the first group of four iterations and three times of the standard deviations in the second and third groups of 6 iterations, excluding the data with large residual during the inversion. We use the conjugate gradient method for solving equations and getting the damped least squares solution.

3 Results and analysis

3.1 Error of relocation

The original observation reports did not give location errors, but only an average traveltime residual of 0.35 s after location. After double difference relocation with the conjugate gradient method, the location error in N-S, E-W, and U-D direction is 0.13, 0.12, and 0.17 km on average, respectively, and the average location residual is about 0.1 s. This shows that the location errors and residuals are reduced significantly after relocation.

However, the results from the conjugate gradient method are not very accurate probably because it approximately calculates diagonal elements for the covariance matrix when solving equations and the error estimation of this method relies heavily on the convergence of iteration [20]. Singular value decomposition method can give more accurate error estimation, but is very time-consuming. For this reason, generally the singular value decomposition method is used to relocate partial data and analyze location errors. In this article, we use the singular value decomposition method for location error analysis. We perform four tests and select 100 events randomly each time for relocation using the singular

value decomposition method. The average of location errors of the four tests in N-S, E-W and U-D direction is 0.30, 0.29 and 0.59 km, respectively. These values represent the relocation accuracy of our results.

3.2 Characteristics of aftershock distribution

Figure 4 shows the relocated epicenter distribution. Compared with the original location results, the relocated epicenter distribution is more concentrated. As seen from Figure 4, the aftershocks are distributed mainly in the NNE direction along both sides of the Shuangshi-Dachuan fault. A few earthquakes occurred in the southern part of aftershock zone but more in the middle-northern part. The magnitudes of earthquakes in the southern aftershock zone are large, and most of the aftershocks occurred on April 20. Aftershocks occurring from April 21 to 27 are mainly in the middle-northern part of the source region. The width of aftershocks distribution changes near Lushan, being wider in the north of Lushan, about 16 km, but only about 8 km in the south of Lushan. It can be found that aftershocks are mainly in the Mesozoic and Cenozoic basins and fewer in the mountain area.

Figure 5 displays the relocated focal depth distribution in different profiles. The positions of the profiles are shown in Figure 4. As viewed from the focal depth profiles, the rupture length is about 35 km and the rupture width is about 16 km. Ninety percent of aftershocks mainly distribute in the depth range of 10–20 km. A few earthquakes occurred in the shallow crust. Within a week after the earthquake, the depth of aftershocks reduced from 16.1 to 13.7 km on average, showing an overall shallowing trend (Figure 6).

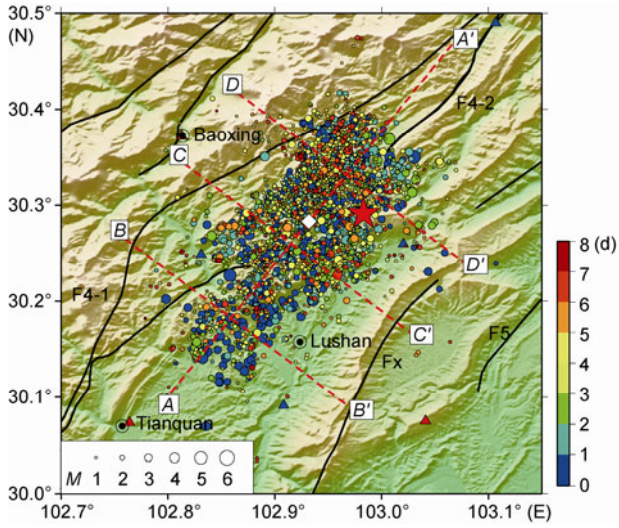

Figure 4 Relocated aftershock epicenter distribution. White square on the profile *AA′* indicates the center of the section. Other legends are the same as in Figure 3.

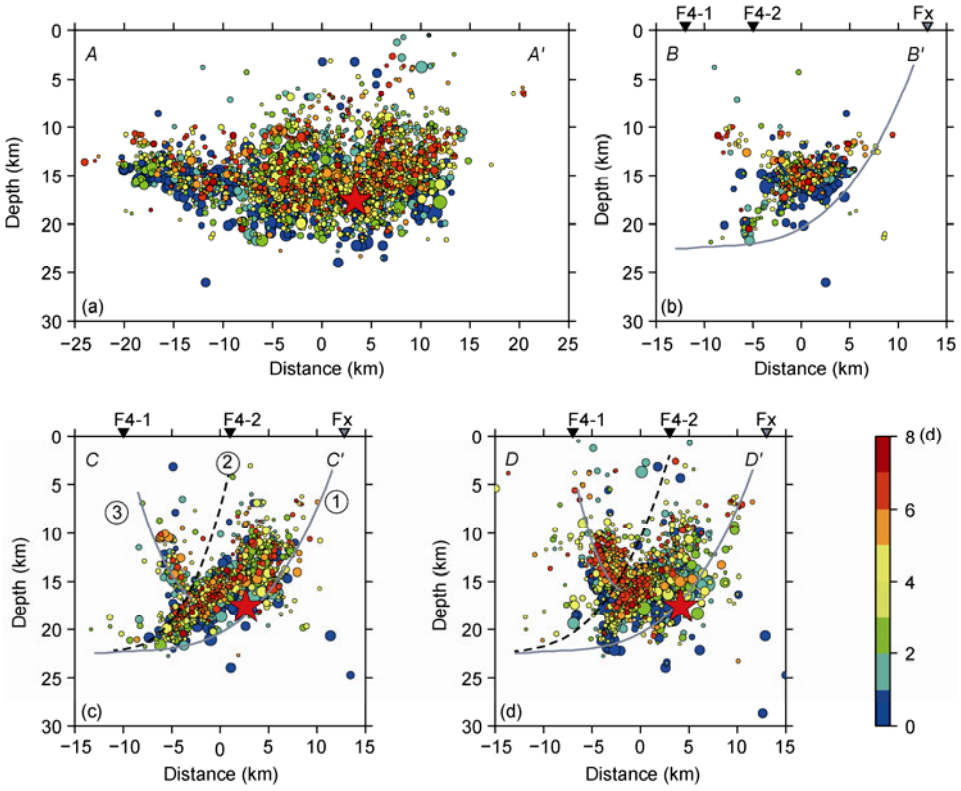

Figure 5 Focal depth profiles. Gray real line ①, ③ represent the deduced shape of seismogenic fault and back thrust fault. Black dashed line ② represents the deduced shape of Shuangshi-Dachuan branch fault. The triangles on the surface indicate the outcrops of the faults. Other legends are the same as in Figure 3. The distance between each earthquake and the axis of the cross-section is less than 6 km.

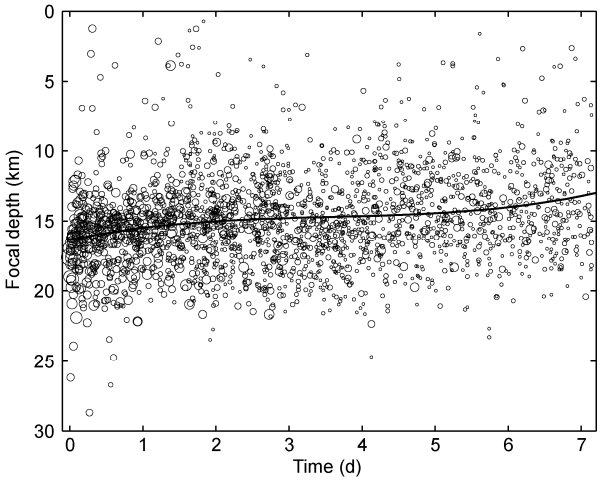

Figure 6 Focal depth changes over time. Black line represents the averages of focal depth in different time periods.

Focal depth along the profile AA' changes significantly. As divided by the abscissa −10 km, focal depth on the left is shallow with a few aftershocks, and focal depth on the right is deep with more aftershocks. Focal depth shows an overall feature that it is shallow in the southwest but deep in the northeast. Profiles BB', CC', DD' show that aftershocks are northwestward dipping and the dip angle is steep in the shallow depth, but gentle at greater depth, manifesting itself as listric fault characteristics.

3.3 Focal depth

After the earthquake, different agencies at home and abroad quickly give the focal depth of Lushan earthquake, but these results show some differences. The focal depth from China Earthquake Networks Center is 13 km. USGS initially gives the focal depth of about 12.3 ± 3.4 km and amends to 14 km later. The focal depth determined using a 3-D velocity model and the double difference algorithm is 17.2 and 17.6 km, respectively. The differences of focal depth are mainly due to sparse station distribution, lack of sufficient data from near stations, leading to poor constraints on the focal depth. The 3-D velocity model used in this study is close to real velocity structure in the epicenter area, and the locations of early aftershocks are corrected using temporal stations. Therefore, we believe that the focal depth given in this paper is more reliable.

The average depth of relocated earthquakes is 14.9 km, and about 85% of the events distribute in the 10–20 km depth range (Figure 7). Sun et al. determined the focal depth of 28 aftershocks with M_L larger than 4.0 using waveform data recorded by China Array and sPn phases (personal communication). Their results show that focal depths of most aftershocks range from 9 to 18 km, which is consistent with the results given in this article.

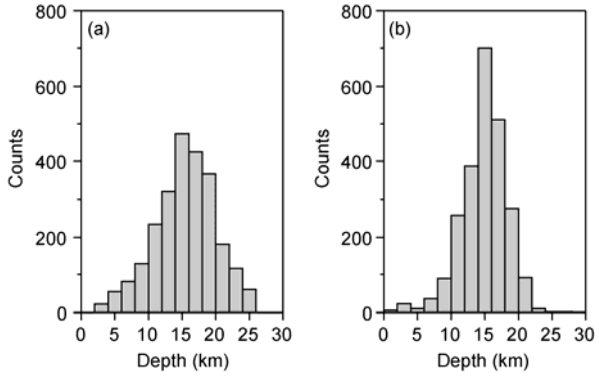

Figure 7 Histogram of focal depth distribution. Before (a) and after (b) earthquake relocation.

4 Discussion

Lushan earthquake occurred in the southern part of the Longmenshan fault zone. The fault system is very complex in this region and is composed of the back fault, central fault, front fault and Dayi fault and so on (Figure 1). Is the seismogenic structure of Lushan earthquake at the Dayi fault in the east of the earthquake region, or the Shuangshi-Dachuan fault region where aftershocks and major surface destruction have apparently occurred, or other active faults? Since the earthquake did not cause significant surface rupture, the seismogenic structure of Lushan earthquake remains controversial. The relocation results show that the aftershocks distribute mainly along both sides of the Shuangshi-Dachuan fault. But further analysis of the spatial distribution of aftershocks is needed to determine the seismogenic fault of Lushan earthquake.

Focal depth profiles of the aftershocks show the seismogenic fault dips northwest, with steep angle in the shallow depth and a gentle angle at greater depth, which shows the listric thrust fault characteristics. In the focal depth profiles, the initial rupture point is located near the outside of the dense aftershock area. According to the focal depth distribution of Lushan earthquake sequence along with the fault data [2–8,13], we determined the morphology of the fault at depth using the least-squares fitting method (Figure 5). The fitting results show that the dip angle of the seismogenic fault is about 63° in the shallow crust, about 41° near the mainshock, and about 17° at the bottom. The focal mechanism inversion results show that the Lushan earthquake is a thrust earthquake, with the strike 220°, dip 35°, and rake angle 95° (http://www.cea-igp.ac.cn/tpxw/266824.shtml). Since the focal mechanism inversion results give the average of the rupture surface solution, the dip angle from focal mechanism inversion can be considered to be consistent with the results inferred from the aftershock distribution in this study.

According to the fitting results of the fault plane, if the seismogenic fault extends to the surface, it can be deduced

that the outcrop of the seismogenic fault is in the east side of the aftershock zone with the distance about 23 km away from Shuangshi-Dachuan fault. Based on the current existing fault data [2–8], there are two faults located on the eastern side of the aftershock area within 40 km, namely the Dayi fault (F6) and an unknown fault (Fx). The distances from the two faults to the Shuangshi-Dachuan fault are 32 and 22 km, respectively. Geological survey shows that there are several buried faults beneath the northwestern margin of the Chengdu Plain. These buried faults are reverse faults with strikes N55°–60°E, dipping to NW [28]. Focal depth profiles of aftershocks clearly depict the Lushan seismogenic structure as a listric thrust fault. According to the aftershock relocation results and the distance between the seismogenic faults and Shuangshi-Dachuan fault, we consider that the seismogenic structure of Lushan earthquake may be a blind thrust fault on the eastern side of Shuangshi-Dachuan fault. The outcrop of the blind fault may be near the Fx fault and the Dayi fault.

The rupture process of Lushan earthquake includes two sub-events [29]. The two sub-events have no apparent rupture direction. There is only a sliding area of 25 km in length and width, and it is mainly distributed nearby the source. The relocation results also show that the focal depth of the mainshock is deeper in the earthquake sequence. However, the fault plane is gentle at greater depth and steep in the shallow depth, and the sizes of the aftershock distribution on both sides of the initiation rupture point along the fault plane are on the same order (Figure 5). This study shows that the mainshock is located beneath the main rupture plane where the dip angle is gentle, indicating that the initial rupture point of the Lushan earthquake is in the deep of the listric thrust fault. The rupture took the initial rupture point as the center and spread around along the fault, but did not reach the surface.

Three focal depth profiles across the source region show that the focal depths of the aftershocks are different between the northern and southern parts. Figure 5 shows that besides the NW dipping aftershock cluster, there is another aftershock cluster dipping to SE. The two clusters can be seen very clear in the *CC′* and *DD′* profiles (fault plane ③). The fault plane ③ intersects with the fault planes ① and ②, which lays out as y-shape. The y-shaped structure is a common combined mode in a thrust fault system, which is called back thrust fault [30]. The y-shape faults are found in many thrust structures, such as the Longmenshan fault, Ordos Basin, the Taiwan central thrust fold belt, etc. [31–33]. The relocation results clearly reveal the existence of the back thrust fault in the aftershock zone of the Lushan earthquake. We speculate that the back thrust fault is formed when the main rupture plane is impeded in the sliding process.

The relocation results show the focal depth of the mainshock is 17.6 km, and the aftershocks are mainly distributed in the depth range of 10–20 km. The mainshock is deep and the aftershock distribution is concentrated. A few aftershocks occurred in the shallow crust, suggesting that the surface ruptures caused by the earthquake may not be obvious. This presumption is confirmed by the source rupture process studies and the earthquake emergency investigation. The rupture process study shows that the static slip of the fault plane is mainly concentrated in the depth range of 10–30 km, and the rupture does not reach the surface [29]. The geological survey also found no surface rupture zone near the Dayi fault, Shanglizhen fault, Gaohezhen fault, Shuangshi-Dachuan fault, Yanjing-Wulong fault, and Lushan-Longmenxiang-Taipingzheng (http://www.eq-igl.ac.cn/www root/c_000000090002/d_0976.html).

The aftershocks of the Lushan earthquake are distributed mainly in the Mesozoic and Cenozoic basins. Few aftershocks occurred in the northwestern mountain areas. Geological data indicates that the western and northern sides of the aftershock zone is a large area exposed with Baoxing massif [34,35]. The Baoxing massif is mainly composed of gabbroic gneiss, diorite gneiss, tonalite gneiss, granodiorite gneiss and massive adamellite. The main constituent minerals of Baoxing massif are plagioclase and quartz [35]. The shear strength and frictional strength of the Baoxing massif are great, so it is hard to break or slip. Body wave traveltime tomography results also show that there is high-velocity anomaly in the upper crust near Baoxing massif [15]. Baoxing massif controls the distribution of the aftershocks to a certain extent and prevents aftershocks spreading to the northwest.

Usually the aftershocks of a thrust earthquake are mainly distributed in the hanging wall, and are relatively fewer in the footwall, while the aftershocks of a strike-slip fault are evenly distributed on both sides [15,24,36]. The relocation results show that the focal depths of the aftershocks are deep in the west and shallow in the east, and the aftershock distribution characteristics is similar to the typical thrust earthquake, such as Wenchuan earthquake and Taiwan Chi-Chi earthquake [24,36]. Numerical simulations show that the coseismic deformation of the hanging wall is much larger than the footwall at the same depth with the same distance away from the fault along the listric thrust fault [37]. For this reason, the damages in the hanging wall are often more serious than those in the footwall during an earthquake. Therefore, the casualties and property losses would be more serious in the hanging wall, such as Lushan, Tianquan, Baoxing, but relatively light in the footwall, such as Ya'an, Mingshan.

5 Conclusion

In this study, we relocated the mainshock and aftershock sequences of Lushan earthquake using data recorded by the Sichuan permanent and temporary seismic stations, and obtained 2405 hypocenter locations with high accuracy.

Relocation results show that the earthquake rupture length is about 35 km and rupture width is about 16 km. The hypocenter depth of the mainshock is 17.6 km, and the dominant focal depth ranges from 10 to 20 km. The shallow earthquakes are rare. Most of aftershocks are in the hanging wall while fewer in the footwall. Aftershocks are mainly distributed in the Mesozoic-Cenozoic basins. Baoxing massif prevents the aftershocks spreading to the northwest due to its great shear strength and frictional strength.

Focal depth profiles show that the aftershocks dips to northwest. The dip angle is steep in the shallow depth and gentle at greater depth, which shows the listric thrust fault characteristics. According to the focal depth distribution, we speculate that the seismogenic fault of Lushan earthquake may be a blind thrust fault on the eastern side of the source region. If this blind thrust fault extends to the surface, it may be located near the Fx fault and the Dayi fault. The final confirmation of the seismogenic structure of the Lushan earthquake needs proofs from deep seismic sounding studies and geological surveys. The dip angle of the seismogenic faults is approximately 63° in the shallow crust, about 41° near the source of the mainshock, and about 17° at the bottom of the fault. The initial rupture point of the Lushan earthquake is located in the deep of the listric thrust fault. The rupture took the initial rupture point as the center and spread around along the fault, but did not reach the surface. We speculate that the seismogenic fault of Lushan earthquake, Longmenshan front fault and central fault may converg into a nearly horizontal detachment thrust fault in the deep crust (about 23 km).

The relocation results reveal clearly the existence of the back thrust fault in the Lushan aftershock zone. This back thrust fault intersects with the seismogenic fault as a y-shape structure. We infer that the back thrust fault is formed when the main rupture plane is impeded in the sliding process.

This study only uses the aftershock data within one week after the mainshock. More data will be collected to relocate the aftershocks, for better understanding the features of aftershock sequence and seismogenic structures of the Lushan earthquake.

We thank anonymous reviewers for their valuable suggestions. We also thank the earthquake emergency personnel of the Sichuan Earthquake Administration, the Institute of Geophysics, Chongqing Earthquake Administration, Yunnan Earthquake Administration, who provide the valuable seismic data recorded by the temporal stations. We appreciate the colleagues of Sichuan Earthquake Administration, as well as colleagues from other provinces, for providing a timely and high-quality observation reports. We express our gratitude to Huang Yuan, Gao Jingchun, Du Wenkang and Su Jinrong for their support of this work. We also thank Data Management Centre of China National Seismic Network at Institute of Geophysics, China Earthquake Administration for providing the waveform data and China Earthquake Networks Center for compiling earthquake phase data. We also thank Prof. Yao Huajian for proofreading the manuscript. This work was supported by the National Natural Science Foundation of China (41074068), the National Science and Technology Support Program (2012BAK19B01), China National Special Fund for Earthquake Scientific Research in Public Interest (201308013) and Scientific Investigation of April 20, 2013 M7.0 Lushan, Sichuan Earthquake.

1 Liu J, Yi G X, Zhang Z W, et al. Introduction to the Lushan, Sichuan *M*7.0 earthquake on 20 April 2013 (in Chinese). Chin J Geophys, 2013, 56: 1404–1407
2 Tang R C, Han W B. Active Faults and Earthquakes in Sichuan (in Chinese). Beijing: Seismological Press, 1993. 1–368
3 Deng Q D, Chen S F, Zhao X L. Tectonics, seismicity and dynamics of Longmenshan mountains and its adjacent regions (in Chinese). Seism Geol, 1994, 16: 389–403
4 Zhang P Z, Wen X Z, Xu X W, et al. Tectonic model of the great Wenchuan earthquake of May 12, 2008, Sichuan, China (in Chinese). Chin Sci Bull (Chin Ver), 2009, 54: 944–953
5 Zhang P Z, Xu X W, Wen X Z, et al. Slip rates and recurrence intervals of the Longmen Shan active fault zone, and tectonic implications for the mechanism of the May 12 Wenchuan earthquake, 2008, Sichuan, China (in Chinese). Chin J Geophys, 2008, 51: 1066–1073
6 Jia D, Chen Z X, Jia C Z, et al. Longmen Shan foreland fold and thrust belt of the western Sichuan foreland basin development (in Chinese). Geol J Chin Univ, 2003, 9: 402–409
7 Xu X W, Zhang P Z, Wen X Z, et al. Western Sichuan and its neighboring regions active tectonics and earthquake recurrence model (in Chinese). Seism Geol, 2005, 27: 446–461
8 Chen G G, Ji F J, Zhou R J, et al. Longmen Shan fault zone late Quaternary activity segmentation preliminary study (in Chinese). Seism Geol, 2007, 29: 657–673
9 Liu Q Y, Li Y, Chen J H, et al. Wenchuan M_S8.0 earthquake: Preliminary study of the S-wave velocity structure of the crust and upper mantle (in Chinese). Chin J Geophys, 2009, 52: 309–319
10 Wen X Z, Zhang P Z, Du F, et al. The background of historical and modern seismic activities of the occurrence of the 2008 M_S8.0 Wenchuan, Sichuan, earthquake (in Chinese). Chin J Geophys, 2009, 52: 444–454
11 Zhou S Y. Seismicity simulation in Western Sichuan of China based on the fault interactions and its implication on the estimation of the regional earthquake risk (in Chinese). Chin J Geophys, 2008, 51: 165–174
12 Lei J S, Zhao D P, Su J R, et al. Fine seismic structure under the Longmenshan fault zone and the mechanism of the large Wenchuan earthquake (in Chinese). Chin J Geophys, 2009, 52: 339–345
13 Xu X W, Han Z J, Li C Y, et al. Lushan M_S7.0 earthquake: A blind reserve-fault earthquake. Chin Sci Bull, 2013, 58: 3437–3443
14 Zheng X F, Ouyang B, Zhang D N, et al. Technical system construction of Data Backup Centre for China Seismograph Network and the data support to researches on the Wenchuan earthquake (in Chinese). Chin J Geophys, 2009, 52: 1412–1417
15 Wu J P, Huang Y, Zhang T Z, et al. Aftershock distribution of the M_S8.0 Wenchuan earthquake and three dimensional P-wave velocity structure in and around source region (in Chinese). Chin J Geophys, 2009, 52: 320–328
16 Fang L H, Wu J P, Zhang T Z, et al. 2011 Yunnan Yingjiang M_S5.8 earthquake and its aftershock sequence relocations (in Chinese). Acta Seismol Sin, 2011, 33: 262–267
17 Wang C Y, Han W B, Wu J P, et al. Crustal structure beneath the eastern margin of the Tibetan Plateau and its tectonic implications. J Geophys Res, 2007, 112: B07307
18 Zhao Z, Fan J, Zheng S H, et al. Crustal structure and accurate hypocenter determination along the Longmenshan Fault zone (in Chinese). Acta Seismol Sin, 1997, 19: 615–622
19 Wang C Y, Lou H, Yao Z X, et al. Crustal thicknesses and poisson's ratios in Longmenshan mountains and adjacent regions (in Chinese). Quat Sci, 2010, 30: 652–661
20 Waldhauser F, Ellsworth W L. A double-difference earthquake location algorithm: Method and application to the Northern Hayward Fault, California. Bull Seismol Soc Am, 2000, 90: 1353–1368
21 Yang Z X, Chen Y T, Zheng Y J, et al. Double-difference earthquake location method in our Midwest earthquake precise positioning ap-

plication (in Chinese). Sci China Ser D-Earth Sci, 2003, 33(Suppl.): 129–134
22 Yu X W, Chen Y T, Wang P D. Three-dimensional P-wave velocity structure in Beijing-Tianjin-Tangshan area (in Chinese). Acta Seismol Sin, 2003, 25: 1–14
23 Zhu A L, Xu X W, Zhou Y S, et al. Relocation of small earthquakes in western Sichuan, China and its implications for active tectonics (in Chinese). Chin J Geophys, 2005, 48: 629–636
24 Huang Y, Wu J P, Zhang T Z, et al. Wenchuan 8.0 earthquake and its aftershocks relocation. Sci China Ser D-Earth Sci, 2008, 38: 1242–1249
25 Chen H L, Zhao C P, Xiu J G, et al. Study on precise relocation of Longtan reservoir earthquakes and its seismic activity (in Chinese). Chin J Geophys, 2009, 52: 2035–2043
26 Zheng Y, Ma H S, Lu J, et al. Source mechanism of strong aftershocks (M_S≥5.6) of Wenchuan earthquake and the implication for seismotectonic (in Chinese). Sci China Ser D-Earth Sci, 2009, 39: 413–426
27 Chen J H, Liu Q Y, Li S C, et al. Seismotectonic study by relocation of the Wenchuan M_S8.0 earthquake sequence (in Chinese). Chin J Geophys, 2009, 52: 390–397
28 Monitoring and Prediction Division, China Earthquake Administration. Wenchuan 8.0 Earthquake Research Reports (in Chinese). Beijing: Seismological Press, 2009. 1–216
29 Zhang Y, Xu L S, Chen Y T. Rupture process of the Lushan 4.20 earthquake and preliminary analysis on the disaster-causing mechanism (in Chinese). Chin J Geophys, 2013, 56: 1408–1411
30 Zhu Z C. Structural Geology (in Chinese). Beijing: China University of Geosciences Press, 1999. 1–273
31 Suppe J. Principles of Structural Geology. J Struct Geol, 1985, 8: 1–721
32 Jin W Z, Tang L J, Yang K M, et al. Deformation and zonation of the Longmenshan fold and thrust zone in the western Sichuan basin (in Chinese). Acta Geol Sin, 2007, 81: 1072–1080
33 Luo Q. Characteristics of faults in Majiatan area of west Ordos basin and their petroleum reservoir controlling model (in Chinese). Acta Geos Sin, 2008, 29: 619–627
34 Xu Z Q, Li H Q, Hou L W, et al. Uplift of the Longmen-Jinping orogenic belt along the eastern margin of the Qinghai-Tibet Plateau: Large-scale detachment faulting and extrusion mechanism (in Chinese). Geol Bull China, 2007, 26: 1262–1276
35 Liu S W, Yang K, Li Q G, et al. Petrogenesis of the Neoproterozoic Baoxing Complex and its constraint on the tectonic environment in western margin of Yangtze Craton (in Chinese). Earth Sci Front, 2009, 16: 107–118
36 Chien H C, Yih M W, Tzay C S, et al. Relocation of the 1999 Chi-Chi Earthquake in Taiwan. Terr Atmos Oceanic Sci, 2000, 11: 581–590
37 Tao W, Hu C B, Wan Y G, et al. Dynamic modeling of thrust earthquake on listric fault and its inference to study of Wenchuan earthquake (in Chinese). Chin J Geophys, 2011, 54: 1260–1269